



Membrane order parameters for interdigitated lipid bilayers measured via polarized total-internal-reflection fluorescence microscopy



An T. Ngo^{a,b}, Zygmunt J. Jakubek^a, Zhengfang Lu^a, Béla Joós^b, Catherine E. Morris^c, Linda J. Johnston^{a,*}

^a Measurement Science and Standards, National Research Council Canada, Ottawa, ON K1A 0R6, Canada

^b Department of Physics, University of Ottawa Ottawa, ON K1N 6N5, Canada

^c Ottawa Hospital Research Institute, Ottawa, ON K1H 8M5, Canada

ARTICLE INFO

Article history:

Received 14 April 2014

Received in revised form 3 July 2014

Accepted 21 July 2014

Available online 26 July 2014

Keywords:

Polarized total internal reflection fluorescence microscopy

Lipid bilayers

Order parameters

Ethanol

Interdigitated phase

ABSTRACT

Incorporating ethanol in lipid membranes leads to changes in bilayer structure, including the formation of an interdigitated phase. We have used polarized total-internal-reflection fluorescence microscopy (pTIRFM) to measure the order parameter for Texas Red DHPE incorporated in the ethanol-induced interdigitated phase ($L_{\beta}I$) formed from ternary lipid mixtures comprising dioleoylphosphatidylcholine, cholesterol and egg sphingomyelin or dipalmitoylphosphatidylcholine. These lipid mixtures have 3 co-existing phases in the presence of ethanol: liquid-ordered, liquid-disordered and $L_{\beta}I$. pTIRFM using Texas Red DHPE shows a reversal in fluorescence contrast between the $L_{\beta}I$ phase and the surrounding disordered phase with changes in the polarization angle. The contrast reversal is due to changes in the orientation of the dye, and provides a rapid method to identify the $L_{\beta}I$ phase. The measured order parameters for the $L_{\beta}I$ phase are consistent with a highly ordered membrane environment, similar to a gel phase. An acyl-chain labeled BODIPY-FL-PC was also tested for pTIRFM studies of ethanol-treated bilayers; however, this probe is less useful since the order parameters of the interdigitated phase are consistent with orientations that are close to random, either due to local membrane disorder or to a mixture of extended and looping conformations in which the fluorophore is localized in the polar headgroup region of the bilayer. In summary, we demonstrate that order parameter measurements via pTIRFM using Texas Red-DHPE can rapidly identify the interdigitated phase in supported bilayers. We anticipate that this technique will aid further research in the effects of alcohols and other additives on membranes.

Crown Copyright © 2014 Published by Elsevier B.V. All rights reserved.

1. Introduction

The effects of alcohols on membranes continue to attract interest due to their implications for human health in areas such as alcohol intoxication, anesthetics and the use of ethanol as a cosolvent for drug delivery [1–3]. Alcohol effects are also relevant to the production of biofuels and specialty chemicals by yeast and bacteria. Many of the consequences of alcohol incorporation are related to changes in the properties and organization of lipid membranes and their embedded proteins [4–6].

Alcohols embedded in lipid membranes orient their hydroxyl moieties near the lipid headgroups [7,8], thus increasing the inter-headgroup spacing in the bilayer. Alcohols with shorter hydrocarbon chains may also create voids between the lipid tails, while those with longer chains

may increase the lateral packing of the membrane [9]. At a threshold concentration that depends on the chain length of the alcohol [10], the increased inter-headgroup spacing causes the lipid tails to interdigitate [7]. Light-scattering [11], X-ray diffraction [7,11,12], and differential scanning calorimetry [11] of vesicle solutions have shown that alcohol-induced interdigitation changes the molecular tilt angle of the lipids, reduces the bilayer thickness, and increases the phase transition temperature. Fluorescence spectroscopy with polarity-sensitive probes has also been used to report on membrane order in the presence of alcohols [13–15].

Atomic force microscopy (AFM) has been used to examine the impact of alcohols on the thickness and mechanical properties of supported lipid bilayers prepared from lipids in either the gel or fluid phase [16, 17]. Adding alcohol to the membrane produces a thinner interdigitated phase of reduced mechanical strength, as evidenced by the force required to break through the bilayer. Recent AFM studies have examined alcohol-treated supported lipid bilayers prepared from ternary lipid mixtures with coexisting liquid-ordered (L_o) and liquid-disordered (L_d) phases [18–20]. Such bilayers provide a model for cellular membranes [21,22]. The AFM work demonstrated the coexistence of interdigitated ($L_{\beta}I$), L_o and L_d phases for some sample compositions, and provided information on the morphology and area fraction of

Abbreviations: AFM, atomic force microscopy; BODIPY-FL-PC, 2-(4,4-difluoro-5,7-dimethyl-4-bora-3a,4a-diaza-s-indacene-3-pentanoyl)-1-hexadecanoyl-*sn*-glycero-3-phosphocholine; Chol, cholesterol; DPPC, dipalmitoylphosphatidylcholine; DOPC, dioleoylphosphatidylcholine; ESM, egg sphingomyelin; $L_{\beta}I$, interdigitated; L_d , liquid-disordered; L_o , liquid-ordered; PBS, phosphate buffered saline; pTIRFM, polarized total internal reflection fluorescence microscopy

* Corresponding author. Tel.: +1 613 990 0973.

E-mail address: Linda.Johnston@nrc-cnrc.gc.ca (L.J. Johnston).

interdigitated phase at a given alcohol concentration. Despite the utility of AFM for monitoring formation of the $L_{\beta}I$ phase, it is challenging to resolve the small height differences between the L_d and $L_{\beta}I$ phases in aqueous ethanol solutions which have higher viscosity than water [23] and require the use of stiffer cantilevers with which it is difficult to image at sufficiently low force to avoid compressing the membrane [18].

As an alternative or complementary technique for rapid identification of the interdigitated phase, Longo and coworkers have demonstrated its labeling by Texas Red DHPE [18]. Fluorescence imaging showed that the $L_{\beta}I$ phase had slightly higher fluorescence intensity than the L_d phase but substantially higher intensity than the L_o phase. The authors hypothesized that the large area expansion caused by interdigitation allows the $L_{\beta}I$ phase to accommodate the bulky Texas Red fluorophore in the polar headgroup region of the bilayer.

To further probe the characteristics of the interdigitated phase, we turned to polarized total-internal-reflection fluorescence microscopy (pTIRFM). The fluorescence intensity of a membrane-embedded dye is measured upon excitation by light of different polarization angles, and an order parameter is calculated which is related to the tilt of the dye with respect to the bilayer normal [24–26]. Recently this technique was used in conjunction with AFM [27] to investigate effects of membrane-active peptides on lipid bilayer reorganization [28] and the restructuring of lipid bilayers in response to enzymatic ceramide generation [29]. It is possible to obtain order parameters with other techniques such as NMR, infrared spectroscopy, small angle X-ray scattering, linear dichroism, and fluorescence anisotropy [30–33]. However, because pTIRFM is an imaging technique, it allows the correlation of order parameters with specific features in a sample. Nevertheless, it is important to note that pTIRFM measures an order parameter of the fluorophore, and so the information on the lipid membrane order is indirect.

In this study, we employ pTIRFM to measure the order parameter of two different dye-labeled lipids (Texas Red DHPE and BODIPY-FL-PC) incorporated into lipid bilayers deposited from ethanol/buffer solution onto mica substrates. Bilayers are prepared from ternary lipid mixtures of dioleoylphosphatidylcholine (DOPC), cholesterol (Chol) and either egg sphingomyelin (ESM) or dipalmitoylphosphatidylcholine (DPPC); similar mixtures are frequently used as a model for the plasma membrane of mammalian cells. The two probes differ in the location of the fluorophore and its orientation with respect to the bilayer normal. The tail-labeled BODIPY-FL-PC adopts a position along the bilayer normal in non-interdigitated lipid bilayers [34]; its orientation has previously been characterized by pTIRFM and by molecular dynamics simulations [27,35,36]. By contrast, the headgroup-labeled Texas Red DHPE is expected to orient with its dipole moment nearly perpendicular to the bilayer normal. We demonstrate that measurement of order parameters via pTIRFM can be used to identify the interdigitated phase in supported lipid bilayers, and that the $L_{\beta}I$ phase is significantly more ordered than either the L_o or L_d phase of bilayers formed from ternary lipid mixtures in the presence of alcohol.

2. Materials and methods

2.1. Materials

Dipalmitoylphosphatidylcholine (DPPC), egg sphingomyelin (ESM), and cholesterol (Chol) were obtained in powder form and dioleoylphosphatidylcholine (DOPC) as a chloroform solution from Avanti Polar Lipids (Alabaster, AL, USA). Texas Red (1,2-dihexadecanoyl-*sn*-glycero-3-phosphoethanolamine, triethylammonium salt) and BODIPY-FL-PC ((2-(4,4-difluoro-5,7-dimethyl-4-bora-3a,4a-diaza-*s*-indacene-3-pentanoyl)-1-hexadecanoyl-*sn*-glycero-3-phosphocholine) were obtained from Invitrogen Life Technologies (Carlsbad, CA, USA). Solutions were maintained at pH 7.3–7.5 with phosphate buffered saline, PBS (137 mM NaCl, 2.7 mM KCl, 10 mM Na_2HPO_4 , 1.8 mM KH_2PO_4).

2.2. Bilayer preparation

The lipids were dissolved in chloroform or 3:1 chloroform/methanol (in the case of ESM) and combined in the following proportions: DOPC/ESM/Chol (2:6:1 molar ratio) and DPPC/DOPC (4:1 molar ratio) + 20 mol% Chol. The fluorescent dyes were dissolved in methanol and added to the lipid mixtures at 0.5 mol%. The solvent was evaporated by blown argon, and the lipid films were dried under vacuum overnight. Films were stored at -20°C for up to 1 week.

The lipids were deposited onto mica-on-glass substrates (see details on substrate preparation in Section 2.4) by vesicle fusion. Fresh vesicles were prepared on the day of each experiment. The dry lipid films were hydrated with 20 vol.% ethanol in PBS to a lipid concentration of 0.5 mg/mL, vortexed for ~5 s to dissolve the lipids, and sonicated for 60 min at 50–65 $^\circ\text{C}$ in a closed container to prevent evaporation. Meanwhile, 20-mL aliquots of ethanol/PBS (1 per sample) were warmed to 45.5 $^\circ\text{C}$.

Into each cell was placed 680 μL warm ethanol/PBS + 120 μL of 0.5 mg/mL lipids, in that order. To minimize evaporation, the cells were placed in closed plastic boxes with a wet Kimwipe and incubated for 5 min at 45.5 $^\circ\text{C}$, and then rinsed with warm ethanol/PBS (about 20 mL) to remove excess vesicles. The cells were returned to the oven and subjected to the following heating/cooling cycle: Heat to 45.5 $^\circ\text{C}$ @ 70 $^\circ\text{C}/\text{h}$. Hold at 45.5 $^\circ\text{C}$ for 15 min. Cool to 39.3 $^\circ\text{C}$ @ 51.6 $^\circ\text{C}/\text{h}$. Cool to 36.2 $^\circ\text{C}$ @ 34.4 $^\circ\text{C}/\text{h}$. Cool to 32.7 $^\circ\text{C}$ @ 22.4 $^\circ\text{C}/\text{h}$. Cool to 29.2 $^\circ\text{C}$ @ 15.9 $^\circ\text{C}/\text{h}$. Cool to 26.8 $^\circ\text{C}$ @ 12.5 $^\circ\text{C}/\text{h}$. Cool to 19.5 $^\circ\text{C}$ @ 8.0 $^\circ\text{C}/\text{h}$. Larger and more reproducible domains are typically formed when vesicle fusion is carried out above the melting temperature for the lipid mixture, and followed by slowly cooling the sample [37,38]. The cells were then washed with 19.5 $^\circ\text{C}$ ethanol/PBS, and sealed with a glass coverslip that had been cleaned with piranha solution and dried with argon.

2.3. Ethanol rinse experiment

DOPC/ESM/Chol bilayers were prepared as above in 20 vol.% ethanol/PBS and imaged. Each sample was then rinsed with at least 20 mL PBS to remove ethanol, incubated 90 min at 20 $^\circ\text{C}$, and imaged again. To replace the ethanol, each sample was rinsed with at least 20 mL of ethanol/PBS, incubated 90 min at 20 $^\circ\text{C}$, and imaged. Finally, to approximately mimic the temperature cycle used in direct deposition of vesicles from ethanol solution, each sample was heated to 45.5 $^\circ\text{C}$ at 90 $^\circ\text{C}/\text{min}$, held at this temperature for 5 min, cooled to 19.5 $^\circ\text{C}$ at 60 $^\circ\text{C}/\text{min}$, and imaged.

2.4. Polarized total internal reflection fluorescence microscopy

Polarized light can be used to determine the orientational order of membrane components because fluorophore excitation is dependent on the reporter's molecular orientation with respect to the polarization of the exciting light [24,27]. In TIRF microscopy fluorophores are excited by an evanescent field generated by total internal reflection of the illuminating light at the substrate/water interface. Because the polarization state of the evanescent field depends, among other factors, on the polarization of the illuminating beam, the orientational order of fluorophores embedded in a supported membrane can be probed by measuring the intensity of fluorescence as a function of the illuminating beam polarization angle. Fluorescent molecules are excited most efficiently when the electric field of the evanescent wave is aligned with their absorption dipole moments. Fluorophores oriented at different tilt angles relative to the substrate normal θ_c will therefore be preferentially excited at different polarization angles. For a planar solid-supported membrane the possible probe tilt angles range from 0 $^\circ$ to 90 $^\circ$ meaning that the order parameter $\langle P_2 \rangle$ ranges from -0.5 to 1.0, where

$$\langle P_2 \rangle = \frac{1}{2} \left(3 \left[\cos^2(\theta_c) \right] - 1 \right)$$

and the average tilt angle ($\langle\theta_c\rangle$) can be calculated from pTIRFM images [39]. An isotropic or randomly oriented distribution of molecules will yield $P_2 = 0$, whereas absorption dipoles randomly oriented perpendicular (parallel) to the membrane normal correspond to the P_2 value of -0.5 (1.0), respectively. The time- and ensemble-averaged orientational order parameter P_2 can be expressed in terms of the fluorescence-detected dichroic ratio, which is an experimentally measured (on a pixel-by-pixel basis) ratio of background-corrected images measured with p and s polarized excitation.

Polarized excitation TIRF microscopy was conducted with a through-the-objective TIRF microscope built on an IX-81 Olympus frame using a $150\times$ (UAPO150XO/TIRFM) Olympus TIRF objective. Fluorophores were excited at either 488 nm with an Ar-ion laser (CVI Melles Griot) or 543 nm with a He-Ne laser (CVI Melles Griot) both coupled with the microscope via a polarization maintaining fiber. Fluorescence was filtered with emission filters FF01-536/40 and FF01-624/40 (Semrock, Rochester, USA) for BODIPY-FL-PC and Texas Red DHPE, respectively. Images were recorded with an EMCCD camera (Cascade 512B, Photometrics). Laser beams were linearly polarized before entering the microscope. Direction of the polarization of the excitation beam was controlled with a Thorlabs zero-order half-wave plate (WPH05M-488 and WPH05M-546 for 488 and 543 nm excitation, respectively) mounted in a home-built mount installed in a filter slot under the objective lens and could be manually set at the required angle around the optical axis of the objective with 1° precision.

Bilayer samples were prepared and imaged at room temperature ($18\text{--}22^\circ\text{C}$) on mica-on-glass substrates, which were freshly prepared as follows and stored in a nitrogen box for no longer than a few days. Number 1 or 1.5 cover slips (Fisher Scientific) were cleaned in Piranha solution, washed with MilliQ water, and dried with dry nitrogen. Thin round sheets of mica (1 in. diameter), typically $10\text{--}15\ \mu\text{m}$ thick, were freshly cleaved and glued to the cover glass with $\sim 2\ \mu\text{L}$ of optical quality glue (NOA 88, Norland Products, Cranbury, NJ) transferred to the glass with particular care to avoid air bubble formation. By gently pressing on the mica sheet, a uniform $\sim 2\ \mu\text{m}$ thick layer of glue was formed, which was subsequently cured by placing the layered substrate under a UV lamp for 30 min.

Cured substrates were examined under a microscope and those with air bubbles, impurities or uneven glue thickness were discarded. Finally, substrates of satisfactory quality were examined with linearly polarized light under a microscope and the direction of the b optical axis of mica in the central region of the substrate was marked. It should be noted that even in high quality mica there exist zones in the cleaved mica sheets oriented at angles to each other. Substrates with excessive zoning were eliminated. Prior to sample preparation, the substrates were washed in 70% ethanol and deionized water.

Mica is a birefringent material and therefore a light beam propagating at an arbitrary direction splits into ordinary and extraordinary beams, which at the large angles of incidence used in TIRF microscopy may result in a double illumination profile and an unknown state of polarization. Detrimental effects of mica anisotropy could be significantly reduced by using mica that was as thin as possible ($10\text{--}15\ \mu\text{m}$, see above) and aligning the b mica axis in the plane of incidence.

All pTIRFM image processing and analysis were done using the National Institutes of Health ImageJ program (<http://rsb.info.nih.gov/ij>). Order parameter maps were calculated [27] using a macro provided by Drs. John Oreopoulos and Christopher M. Yip (University of Toronto, Canada) with the incidence angle $\alpha = 60^\circ$, sample refractive index $n_1 = 1.3326$ (water), and the substrate refractive index $n_2 = 1.5750$ (mica, average). Order parameters were obtained by averaging data from multiple cross sections for two or more images for multiple samples in most cases.

3. Results

3.1. Intensity changes with polarization of incident light

Supported lipid bilayers were prepared from DOPC, ESM, Chol mixtures in a 2:6:1 molar ratio with 0.5 mol% Texas Red DHPE and imaged by fluorescence in 20 vol.% ethanol/aqueous PBS buffer (Fig. 1). Our choice of lipid composition was based on the extensive use of similar ternary lipid mixtures as models to study co-existing L_o and L_d phases and the recent observation that ternary lipid mixtures containing Chol generate an interdigitated phase in a Chol-dependent manner [18, 20–22]. Unless otherwise noted, all experiments used 20 vol.% ethanol, above the threshold at which the interdigitated phase is formed [18]. Epifluorescence images recorded with axial illumination (Fig. 1a, b) show large branched domains surrounded by a phase of intermediate intensity that contains a number of small dark regions. Images obtained in pTIRFM mode with s -polarization excitation (Fig. 1c) are similar to those obtained with axial illumination. However, with p -polarization excitation (Fig. 1d), the contrast is reversed and the branched domains are darker than the surrounding brightly fluorescent membrane. Measurement of the fluorescence intensity in defects created in the bilayer indicates that the small dark features observed with both p - and s -polarization illumination have higher intensities than the background and, therefore, do not correspond to bilayer defects. The overall fluorescence intensity for pTIRFM images is higher for s -polarization excitation, which is consistent with the predicted orientation of the transition dipole perpendicular to the bilayer normal. In the case of conventional fluorescence microscopy with axial illumination (eg. Fig. 1a, b) the excitation light is polarized predominantly in the sample ($X\text{--}Y$) plane, and therefore mimics s -polarization excitation in pTIRF (Fig. 1c).

The branched structures in Fig. 1 are assigned to the $L_{\beta}I$ phase by analogy to the combined AFM and fluorescence results obtained by Longo and coworkers [18] for a similar ternary lipid mixture comprised of DPPC/DOPC/ergosterol and imaged with axial illumination. The branched domains are surrounded by the L_d phase, with the small dark domains corresponding to the L_o phase. To support this assignment and illustrate the generality of the above observations, a DPPC/DOPC/Chol bilayer was imaged by pTIRFM (Fig. 2). This ternary lipid mixture also shows branched domains whose contrast reverses with respect to the surrounding bilayer when the excitation is changed from s -polarized to p -polarized. The images in Fig. 2a and b show that the fluorescence intensity was frequently higher around the edges of the branched interdigitated domains (see cross section in Fig. 2d). Brighter edges were observed for a number of bilayers from both ESM and DPPC mixtures, although the differences in intensity were frequently smaller than those shown in Fig. 2. A similar heterogeneity in fluorescence intensity of the $L_{\beta}I$ phase has been reported for DPPC/DOPC/ergosterol mixtures [18].

The change of image contrast upon varying the incident light polarization angle is further illustrated in Fig. 3, where the polarization of the incident light is rotated in 20° increments (Fig. 3a–g) for a DOPC/ESM/Chol bilayer. The relative contrast reversal between the liquid-disordered and interdigitated phase with variation of polarization is evident in Fig. 3h. Note that the differences in intensity between the two phases are barely detectable in image d, which is close to the point of contrast reversal.

3.2. Measuring the order parameter of the interdigitated phase with Texas Red DHPE

Fig. 4 shows a representative order parameter map for a DOPC/ESM/Chol bilayer containing Texas Red DHPE, along with the corresponding intensity images obtained under p - (Fig. 4a) and s -polarization (Fig. 4b) excitation. The color scale for the order parameter map varies with increasing parameter value from pink/purple (-0.3) to orange to yellow (-0.15). The same pTIRF experiment was repeated for 4

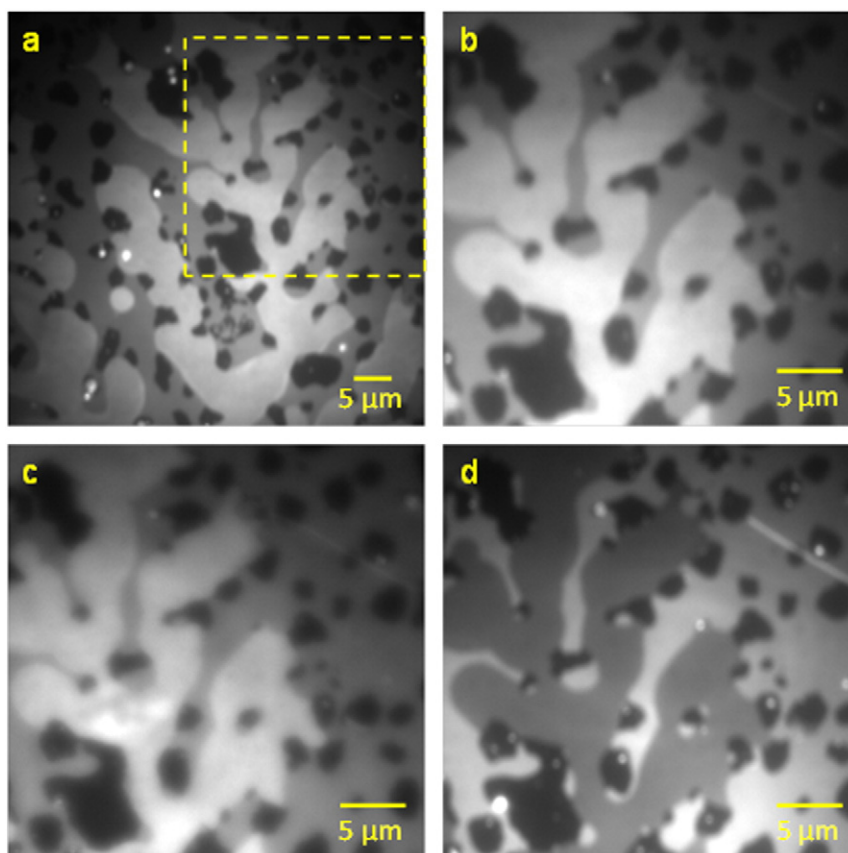


Fig. 1. Fluorescence images of DOPC/ESM/Chol bilayers (2:6:1 molar ratio, 0.5 mol% Texas Red DHPE) illustrating the formation of the ethanol-induced interdigitated phase, $L_{\beta I}$, in 20 vol.% ethanol/PBS. Panel a shows an image obtained with axial illumination. Panel b shows a smaller-scale image of the region outlined in yellow in panel a. Panels c and d show pTIRF images obtained with *s*- and *p*-polarization excitation, respectively, for the same region shown in panel b. They illustrate reversal of contrast between the branched domains that are assigned to the $L_{\beta I}$ phase and the surrounding contiguous L_d phase.

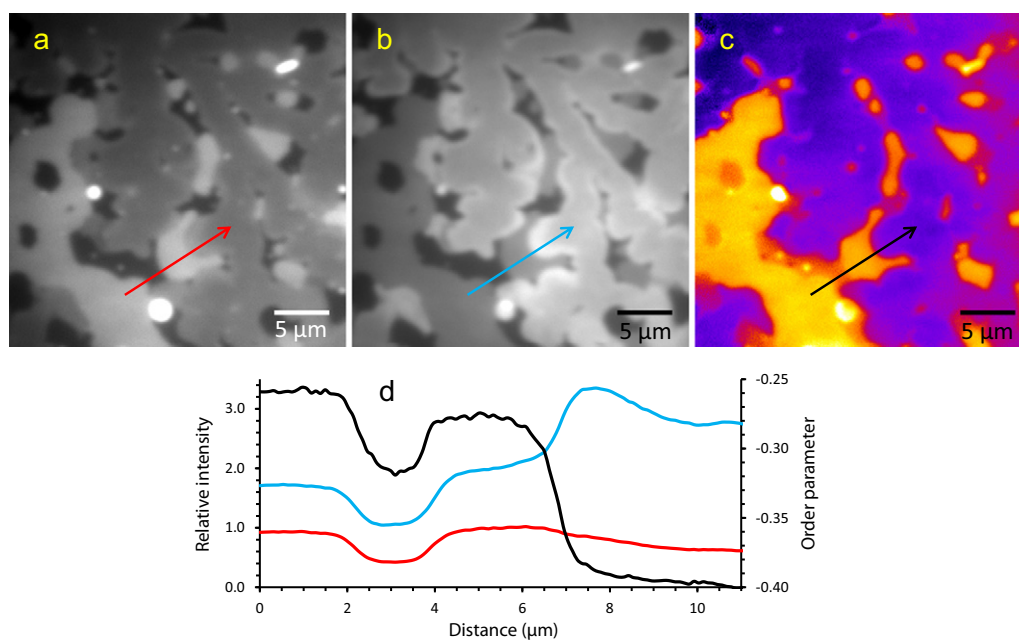


Fig. 2. Fluorescence images of DOPC/DPPC/Chol bilayers (4:1 DOPC/DPPC + 20 mol% Chol with 0.5 mol% Texas Red DHPE) in 20 vol.% ethanol/PBS: (a) *p*-polarization excitation image, (b) *s*-polarization excitation image, (c) order parameter map corresponding to images a and b, and (d) cross-sections along the arrows in panels a, b, and c shown in corresponding colors. The brightness of image a, which was much darker as originally recorded, was increased for clarity. The cross-section traces in panel d show the relative intensities of images a and b as recorded.

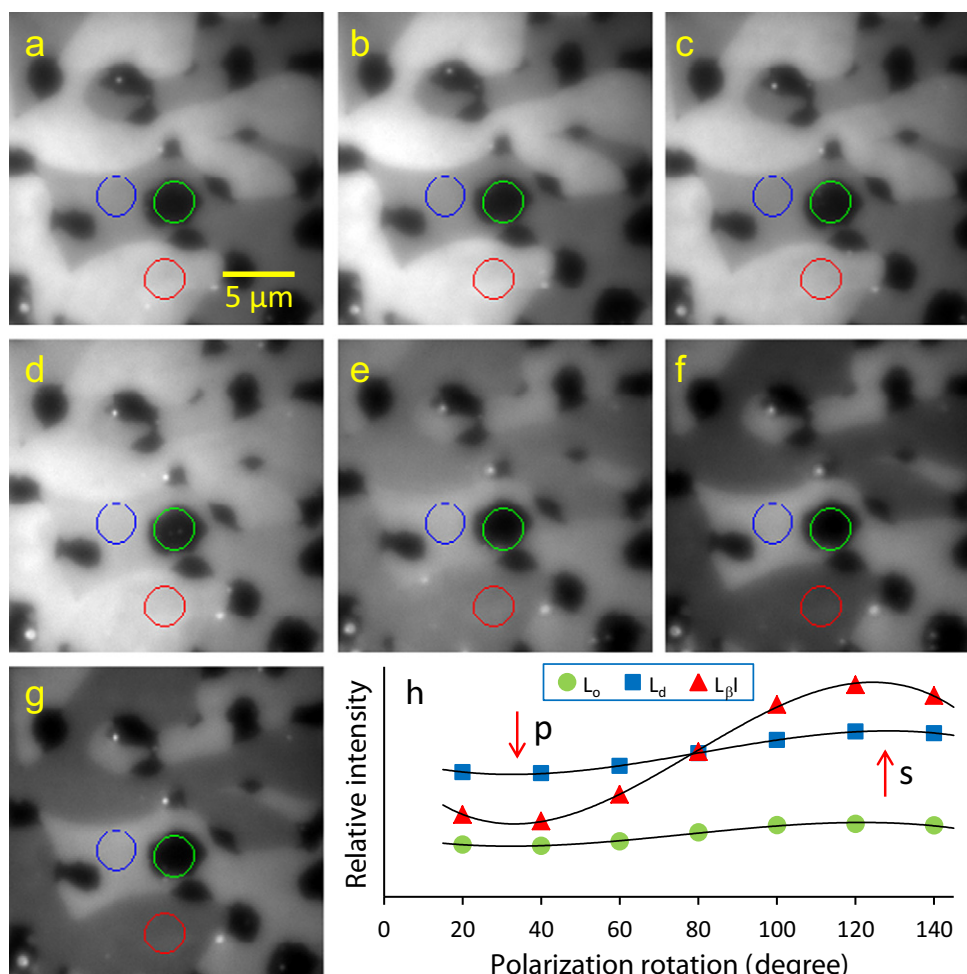


Fig. 3. Contrast evolution in pTIRF images (a–g) of the ethanol-induced interdigitated phase in DOPC/ESM/Chol bilayers with rotation of incident light polarization in 20° increments. Images a–c are on the same intensity scale. Images d–g are on the same intensity scale, which is different from that used for a–c. (h) Average intensity of each phase as measured within the circles marked in images a–g: L_o (green), L_d (blue) and L_{βI} (red). The angles corresponding to *p* and *s*-polarized excitation are indicated with arrows.

independently prepared bilayers; average values for the order parameter, $\langle P_2 \rangle$, and the tilt angle, $\langle \theta_c \rangle$, of the fluorophore transition dipole were obtained from 10 cross-sections per image from 2–5 images per sample (Table 1). The liquid-disordered, liquid ordered and interdigitated phases exhibit order parameters of -0.168 ± 0.025 , -0.228 ± 0.025 , and -0.345 ± 0.026 , respectively, indicating that Texas Red is in a substantially more ordered environment in the interdigitated phase. This further supports our assignment of the branched domains as the L_{βI} phase. The average tilt angle in the L_{βI} phase is approximately 10° closer to perpendicular to the bilayer normal than in the L_d phase.

Order parameters were also determined for a DPPC/DOPC/Chol bilayer in ethanol/buffer, as shown in the order parameter map in Fig. 2c and summarized in Table 1. The trend is similar to that observed for ESM/Chol bilayers in that the L_{βI} phase has a higher order parameter than the L_o phase which is in turn higher than the L_d phase. The order parameter for each phase is higher than the value measured for the bilayers containing ESM. For DPPC/DOPC/Chol the $\langle P_2 \rangle$ value for the L_o phase appears to depend on the surrounding phase. When the L_o domains are predominantly bordered by the L_d phase, their measured $\langle P_2 \rangle$ is -0.312 ± 0.010 (Fig. 2c, black line), corresponding to $\langle \theta_c \rangle = 69.3 \pm 0.6^\circ$. When L_{βI} is the predominantly surrounding phase, the $\langle P_2 \rangle$ of the L_o phase is -0.359 ± 0.005 , corresponding to $\langle \theta_c \rangle = 72.1 \pm 0.3^\circ$. Although the L_{βI} domains exhibit higher fluorescence intensities at their edges, this does not lead to a difference in order parameter between the edges and the interior of these domains (Fig. 2c).

To provide order parameters for the L_o and L_d phase in the absence of ethanol, a pTIRFM experiment was carried out for a DOPC/ESM/Chol (2:2:1 molar ratio) bilayer labeled with Texas Red DHPE and formed and imaged in water. A different lipid ratio from that used for ethanol-treated bilayers was employed because domains formed with the higher ESM mol fraction were too small for quantitative studies by fluorescence microscopy. The order parameters were -0.24 and -0.19 for the L_o and L_d phases, similar to those measured in the presence of alcohol.

3.3. Order parameters measured with BODIPY-PC

For comparison with the results with Texas Red DHPE labeled bilayers, the pTIRF experiments were repeated with BODIPY-PC (Fig. 5), which has been used previously to assess order parameters for L_o and L_d phases in several ternary lipid mixtures [27,29,40]. The absorption dipole moment of the dye moiety of BODIPY-labeled lipid probes has been reported to adopt an orientation nearly parallel to the bilayer normal [27,34]; thus, the order parameters will vary between 0 and 1 for this probe, a wider range than is available with Texas Red-DHPE whose order parameter varies between 0 and -0.5 .

Fig. 5 shows representative images obtained under *p*- and *s*-polarization excitation for a DOPC/ESM/Chol bilayer containing BODIPY-PC in ethanol/PBS (see Supporting Information for a larger image). Both *p*- and *s*-polarization excited images show dark branched domains surrounded by a brighter phase and there is no reversal of

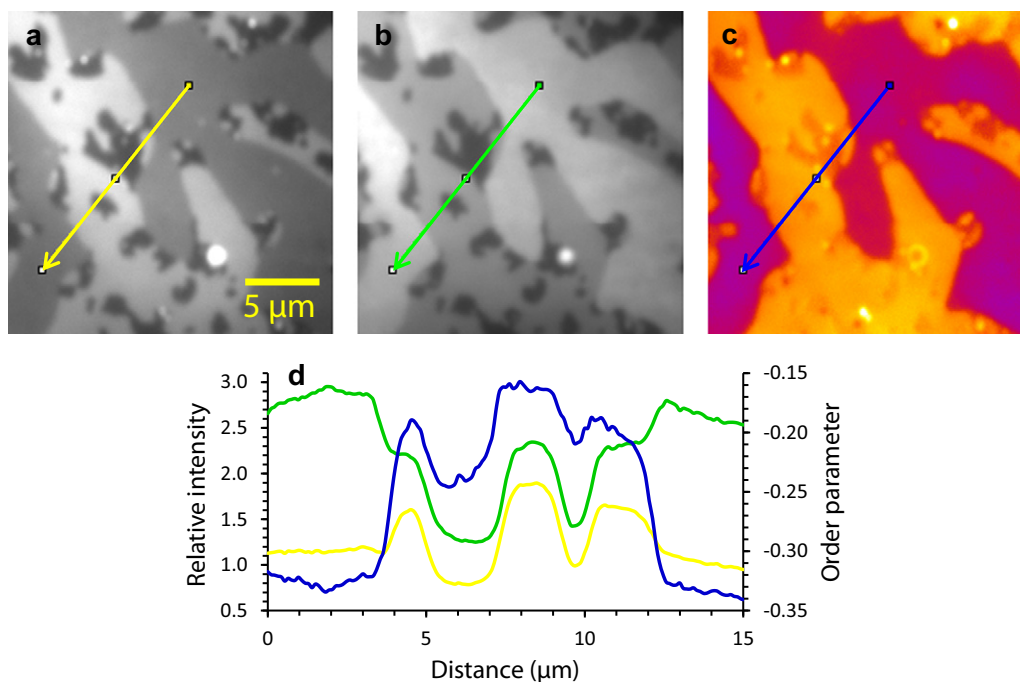


Fig. 4. pTIRF images and an order parameter map for a DOPC/ESM/Chol bilayer containing 0.5 mol% Texas Red DHPE in 20 vol.% ethanol/PBS: (a) *p*-polarization excited image; (b) *s*-polarization excited image; (c) order parameter map; (d) corresponding cross-sections along the yellow, green (left y-axis) and blue (right y-axis) lines in panels a, b and c, respectively.

contrast with change in polarization. The dark branched domains are assigned to the $L_{\beta}I$ phase, by analogy to the results obtained above. The *s*-polarization excited image shows small dark domains of L_o phase but these cannot be distinguished from the $L_{\beta}I$ phase in images obtained with *p*-polarization excitation. A representative order parameter map is also shown in Fig. 5f and data averaged from a total of 11 images from 4 bilayers are shown in Table 1. The order parameters for BODIPY-PC in the L_o and L_d phases are 0.243 ± 0.035 and 0.176 ± 0.027 , respectively. The lower order for the L_d phase is similar to the trend observed with Texas Red and consistent with values obtained in other ternary lipid mixtures with the BODIPY-PC probe (0.28 and 0.20 for L_o and L_d phases, respectively [29]). However, the order parameter in the interdigitated phase, 0.046 ± 0.060 , is significantly lower than in the other phases and varies considerably across the image as evidenced by the high standard deviation, which is approximately twice that obtained for the other two phases. The order parameter value is close to zero, the value that would be obtained for random orientation of the fluorophore. The

high standard deviation is also consistent with a range of orientations of the BODIPY fluorophore in this phase, as discussed in more detail below.

3.4. Effects of varying ethanol concentration

Fig. 6 illustrates the effects of removing and replacing alcohol in the solution above a DOPC/ESM/Chol bilayer; images obtained with *p*- and *s*-polarization excitation and the corresponding order parameter maps are shown for the same bilayer as prepared in 20 vol.% ethanol/PBS, after replacing the solution with PBS buffer and after replacing the buffer with ethanol/PBS. The initial bilayer (Fig. 6a–c) has a similar morphology to the samples shown in Figs. 1 and 3, with branched domains of $L_{\beta}I$ phase that are either brighter or darker than the surrounding L_d phase for *s*- and *p*-polarization excitation, respectively. In Fig. 6d–f, the sample has been rinsed with PBS and incubated for 90 min at 20 °C. The sample morphology has changed dramatically to give large areas that have reasonably uniform fluorescence intensity and no evidence of phase separation as well as dark regions that are similar in intensity to the background. This observation is consistent with loss of ethanol and the interdigitated phase leading to a bilayer that occupies a smaller surface area and has large defects. The order parameter for homogeneous regions of the bilayer is approximately -0.25 , based on Fig. 6f. Replacing the PBS with ethanol/PBS solution and incubating the sample at room temperature leads to a more complex bilayer morphology in which the interdigitated phase cannot be conclusively identified (data not shown). However, after heating above the phase transition temperature of ESM and then cooling to room temperature, the bilayer develops branched domains that resemble the original sample in appearance, contrast reversal behavior, and order parameter (Fig. 6g–i).

DOPC/ESM/Chol bilayers were also formed in the presence of 15 vol.% ethanol/PBS and imaged by pTIRFM. In this case the sample morphologies and the changes in intensity and contrast reversal with variable polarization (data not shown) were qualitatively similar to those observed using 20% ethanol. Although the amount of alcohol incorporated in the interdigitated phase is not known, this control experiment indicates that small changes in ethanol concentration due to evaporation during the bilayer incubation or imaging experiments do

Table 1

Order parameters and tilt angles for Texas Red DHPE and BODIPY-FL-PC partitioned between the L_d , L_o , and $L_{\beta}I$ phases in bilayers of DOPC/ESM/Chol and DPPC/DOPC/Chol in 20 vol.% ethanol/PBS. At least four samples were measured for each of the DOPC/ESM/Chol mixtures and one sample for DPPC/DOPC/Chol. Reported values were averaged from 10 cross-sections per image from at least 2 images per sample, except for DOPC/ESM/Chol labeled with BODIPY, for which the average includes 1 image from each of two samples.

System*	Phase	Order parameter		Tilt angle	
		$\langle P_2 \rangle$	$\Delta \langle P_2 \rangle$	$\langle \theta_c \rangle$ (°)	$\Delta \langle \theta_c \rangle$ (°)
DOPC/ESM/Chol Texas Red DHPE	L_d	-0.168	0.025	61.9	1.2
	L_o	-0.228	0.025	64.8	1.2
	$L_{\beta}I$	-0.345	0.026	71.2	1.6
DPPC/DOPC/Chol Texas Red DHPE	L_d	-0.282	0.022	67.6	1.2
	L_o	-0.335	0.026	70.6	1.6
	$L_{\beta}I$	-0.403	0.010	75.3	0.8
DOPC/ESM/Chol BODIPY-FL-PC	L_d	0.176	0.027	47.8	1.0
	L_o	0.243	0.035	45.3	1.3
	$L_{\beta}I$	0.046	0.060	52.9	2.4

* For comparison, $\langle P_2 \rangle$ values of -0.24 and -0.19 were measured for DOPC/ESM/Chol bilayers labeled with Texas Red in the absence of ethanol.

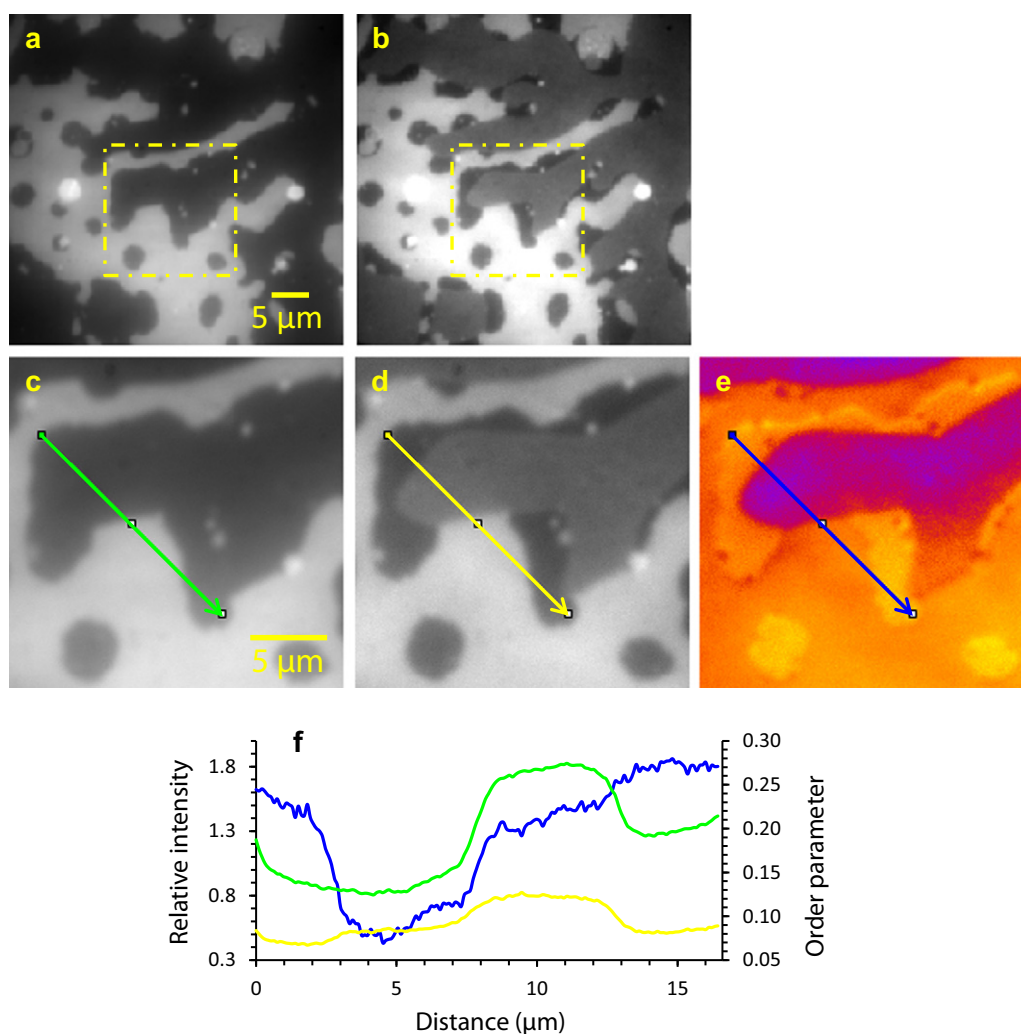


Fig. 5. Representative images and the corresponding order parameter map for a DOPC/ESM/Chol bilayer containing 0.5 mol% BODIPY-PC and imaged in 20 vol.% ethanol/PBS. (a and c) *p*-polarization excited image, full image and the middle area crop, respectively; (b and d) *s*-polarization excited image, full image and the middle area crop, respectively; (e) order parameter map corresponding to images c and d; (f) cross-sections along the lines indicated in images c, d, and e drawn with corresponding colors.

not have a significant effect on the results obtained. The results of the rinsing experiment are consistent with the literature data on the ethanol concentration required for complete formation of $L_{\beta}I$ in several lipid mixtures [18,19]. It should also be noted that although the buffer rinse removes enough ethanol to eliminate the interdigitated phase, there may still be residual alcohol remaining in the bilayer.

4. Discussion

A recent study by Longo and coworkers has shown that Texas Red DHPE can be used to visualize the three coexisting phases (L_0 , L_d , $L_{\beta}I$) in supported lipid bilayers prepared from ternary lipid mixtures in the presence of ethanol [18]. The $L_{\beta}I$ and L_d phases had similar fluorescence intensities, in contrast to the strong preference of Texas Red DHPE to partition into liquid-disordered phases rather than ordered domains. The authors concluded that the area expansion of the bilayer caused by interdigitation can accommodate the large headgroup of Texas Red-DHPE [18]. In the present study we have demonstrated that pTIRFM provides advantages over conventional fluorescence microscopy for the visualization and characterization of the interdigitated phase. The utility of Texas Red-DHPE is not limited to the initial DPPC/DOPC/ergosterol system studied by Longo since it can also be used to visualize three coexisting phases for the two ternary lipid mixtures studied here. More importantly, pTIRFM can be used to measure order parameters

and fluorophore tilt angles, providing useful information on the order of the surrounding bilayer membrane. There is a reversal in contrast between the $L_{\beta}I$ and L_d phases as the polarization of the excitation light is varied, which allows one to select the polarization angle that gives the maximal contrast in fluorescence intensity between phases and provides a rapid method of identifying the $L_{\beta}I$ phase. This may be an advantage for studying the evolution of the $L_{\beta}I$ phase as a function of time or ethanol concentration and for measuring phase diagrams by fluorescence microscopy. Furthermore, the contrast reversal between $L_{\beta}I$ and L_d phases clearly illustrates the fact that one cannot use fluorescence intensities as a measure of probe partitioning for supported bilayers even using conventional fluorescence microscopy. This is because axial illumination results in polarization of the excitation beam predominantly in the sample plane (as noted above) and therefore the intensity varies with changes in probe orientation. Although this observation has been noted in some studies of partitioning of fluorescent probes in bilayer membranes [41], it is not always taken into account. Finally, it is tempting to speculate that the high degree of orientation order for the Texas Red DHPE is related to its ability to partition into this phase. However, a partition coefficient would be required to confirm this hypothesis.

The order parameters measured by pTIRFM indicate that the $L_{\beta}I$ phase is significantly more ordered than either the L_0 or L_d phase for both ESM and DPPC-containing bilayers. The overall $\langle P_2 \rangle$ trend of $L_d <$

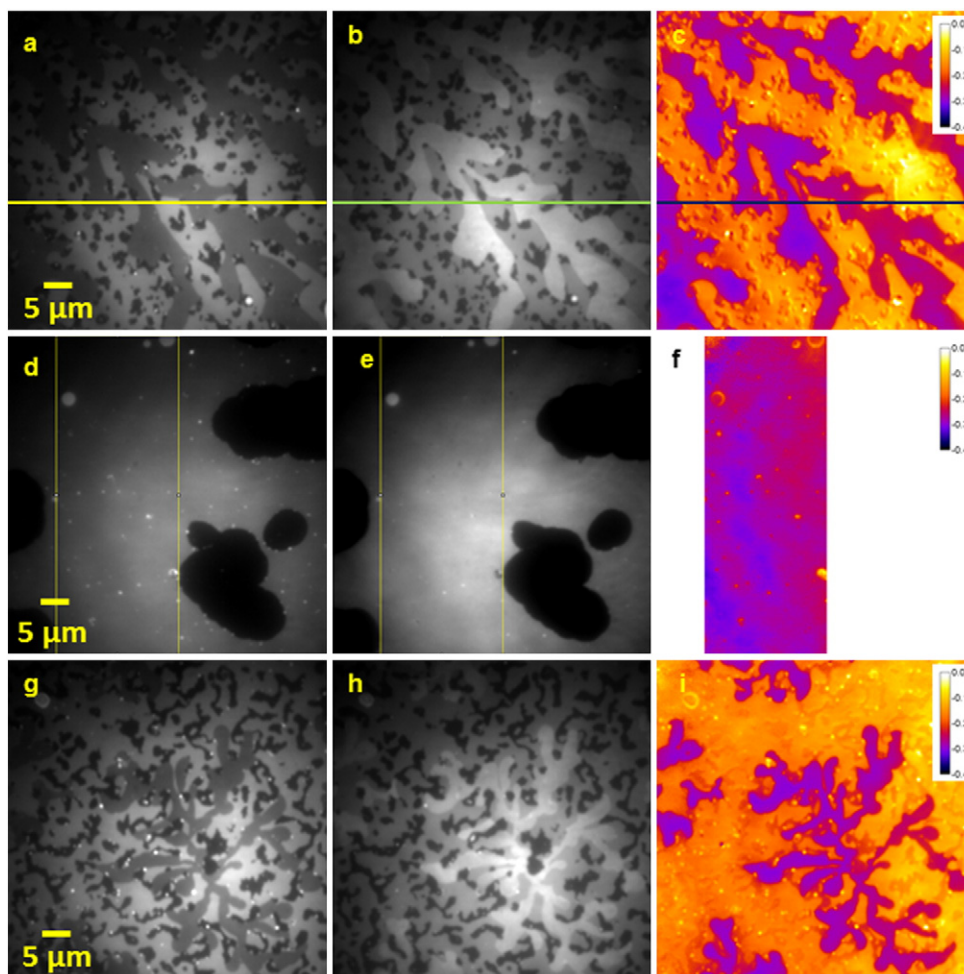


Fig. 6. Changing the ethanol concentration in the solution above the bilayer leads to the disappearance/reappearance of the interdigitated phase. (a–c) A DOPC/ESM/Chol bilayer with 0.5 mol% Texas Red DHPE, freshly deposited from 20 vol.% ethanol/PBS; (d–f) the same bilayer (different region) after rinsing with PBS to remove ethanol and incubating for 90 min at 20 °C; (g–i) the bilayer was rinsed with ethanol/PBS and incubated for 90 min at 20 °C (results not shown) and then heated rapidly to 45.5 °C at 90 °C/min, maintained at that temperature for 5 min, and cooled to room temperature and reimaged. Panels a, d, and g were obtained with *p*-polarization excitation, panels b, e, and h with *s*-polarization excitation, and panels c, f and i are the corresponding order parameter maps (only the defect-free region of the bilayer is shown for panel f).

$L_0 < L_{\beta I}$ is consistent with several previous pTIRFM studies of coexisting L_0 and L_d phases in supported bilayers using BODIPY-PC and a head-group-labeled NBD-ceramide probe [27,29] and with a fluorescence polarization microscopy study in giant unilamellar vesicles using a BODIPY-labeled cholesterol probe [40]. The trend is also in agreement with our recent observation of a high order parameter (relative to the L_0 phase) for ceramide-enriched phases formed by enzymatic hydrolysis of SM in ESM/DOPC/Chol bilayers [29]. Similarly, a recent fluorescence anisotropy study concluded that the lipid order of a DPPC/butanol $L_{\beta I}$ phase is similar to that of the DPPC gel phase [42]. X-ray and neutron scattering have also been used to probe the effects of ethanol on fluidity and permeability of DMPC membranes [8]. Ethanol incorporation led to a stiffer and better-ordered structure for gel phase membranes and to a 50% decrease in lipid diffusion, but had minimal effects on the fluid phase. Order parameters for membranes exposed to short chain alcohols have been measured by electron spin resonance with spin-labeled probes or by ^2H NMR [43–45]. These experiments showed a reduction in membrane order after the incorporation of relatively low concentrations of alcohol for membranes in a fluid/liquid-disordered phase. A similar disruption of lipid packing has been observed after addition of low concentrations of ethanol to ternary lipid mixtures that are models for stratum corneum membranes [46]. However, since measured order parameters depend on both the probe and method used, only qualitative agreement in trends can be expected when comparing various experiments.

We have also examined the utility of BODIPY-PC for pTIRFM studies of the interdigitated phase. The differences between the L_0 and $L_{\beta I}$ phases cannot be distinguished using *s*-polarized excitation, which is comparable to the axially illuminated illumination that is used for most fluorescence imaging. Similar behavior was reported for an acyl-chain labeled probe, NBD-PC, in DPPC/DOPC/ergosterol mixtures [18]. However, all 3 phases can be distinguished with BODIPY-PC using *p*-polarized excitation and the order parameters for the L_0 and L_d phases in DOPC/ESM/Chol bilayers are comparable to those measured previously [27,29]. By contrast, the order parameter for the $L_{\beta I}$ phase is close to zero (0.04), indicating that, on average, the fluorophore is approximately randomly oriented in the interdigitated phase. This suggests that the tightly packed interdigitated phase is unable to accommodate the acyl-chain labeled probe without introducing significant disorder. There are two possible explanations for this observation: a high degree of local disorder in adjacent lipids for an extended conformation of the probe in which the fluorophore is aligned with the lipid acyl chains, or a looping conformation in which the fluorophore moves into the polar headgroup region of the bilayer. Precedent for the latter explanation is provided by studies in which mixtures of extended and looping probe orientations have been observed by single-molecule fluorescence for some chain-labeled BODIPY-PC probes in both bilayers and monolayers [35,47]. Nevertheless, our results do not allow us to distinguish between the two possible explanations.

In summary, we demonstrate herein that polarized TIRF microscopy is a powerful tool for the rapid identification and characterization of the interdigitated phase in supported lipid bilayers deposited from ethanol solution. The reversal in contrast observed for several phase-separated bilayers means that it is straightforward to adjust the polarization angle for maximum contrast between the various phases, which may find application in measuring phase diagrams and following the formation of interdigitated phases. We also show that probes in which the fluorophore is attached to the lipid head group are more useful for pTIRFM studies of the $L_{\beta}I$ phase since acyl chain labeled probes disrupt the bilayer packing and/or adopt multiple conformations. Finally, pTIRFM provides a quantitative measure of the high degree of order of the interdigitated phase, consistent with expectations from a number of other studies. In fact, the high $\langle P_2 \rangle$ value is a good diagnostic test for the formation of the $L_{\beta}I$ phase and is more reliable than AFM due to the small height difference between $L_{\beta}I$ and L_d phases.

Supplementary data to this article can be found online at <http://dx.doi.org/10.1016/j.bbame.2014.07.020>.

Acknowledgments

This work was supported in part by the CREATE program in Quantitative Biomedicine, funded by the Natural Sciences and Engineering Research Council (NSERC) of Canada. We also acknowledge support from a Vision 2020 postdoctoral fellowship, University of Ottawa (ATN), NSERC Discovery Grants (BJ and LJJ) and the Ottawa Hospital Research Institute (CEM). We thank Dr. J. Oreopoulos and C. M. Yip for the ImageJ macro for pTIRF analysis.

References

- [1] R.P. Jones, Biological principles for the effects of ethanol, *Enzym. Microb. Technol.* 11 (1989) 130–153.
- [2] P. Seeman, The membrane actions of anesthetics and tranquilizers, *Pharmacol. Rev.* 24 (1972) 583–655.
- [3] A.C. Williams, B.W. Barry, Penetration enhancers, *Adv. Drug Deliv. Rev.* 56 (2004) 603–618.
- [4] R.K. Finol-Urdaneta, J.R. McArthur, P.F. Juranka, R.J. French, C.E. Morris, Modulation of KvAP unitary conductance and gating by 1-alkanols and other surface active agents, *Biophys. J.* 98 (2010) 762–772.
- [5] H.L. Ingolfsson, O.S. Andersen, Alcohol's effects on lipid bilayers, *Biophys. J.* 101 (2011) 847–855.
- [6] C. Yuan, M. Chen, D.F. Covey, L.J. Johnston, S.N. Treistman, Cholesterol tuning of BK ethanol response is enantioselective and is a function of accompanying lipids, *PLoS One* 6 (2011) e27572.
- [7] T. Adachi, H. Takahashi, K. Ohki, I. Hatta, Interdigitated structure of phospholipid-alcohol systems studied by X-ray diffraction, *Biophys. J.* 68 (1995) 1850–1855.
- [8] L. Topozzini, C.L. Armstrong, M.A. Barrett, S. Zhang, L. Luo, H. Nanda, V.G. Sakai, M.C. Rheinstadter, Partitioning of ethanol into lipid membranes and its effects on fluidity and permeability as seen by X-ray and neutron scattering, *Soft Matter* 8 (2012) 11839–11849.
- [9] T.H. Aagaard, M.N. Kristensen, P. Westh, Packing properties of 1-alkanols and alkanes in a phospholipid membrane, *Biophys. Chem.* 119 (2006) 61–68.
- [10] E.S. Rowe, Lipid chain length and temperature dependence of ethanol-phosphatidylcholine interactions, *Biochemistry* 22 (1983) 3299–3305.
- [11] U. Vierl, L. Lobbecke, N. Nagel, G. Cevec, Solute effects on the colloidal and phase behavior of lipid bilayer membranes: ethanol-dipalmitoylphosphatidylcholine mixtures, *Biophys. J.* 67 (1994) 1067–1079.
- [12] T. Adachi, A new method for determining the phase in the X-ray diffraction structure analysis of phosphatidylcholine/alcohol, *Chem. Phys. Lipids* 107 (2000) 93–97.
- [13] E.S. Rowe, J.M. Campion, Alcohol induction of interdigitation in distearoyl-phosphatidylcholine: fluorescence studies of alcohol chain length requirements, *Biophys. J.* 67 (1994) 1888–1895.
- [14] J. Zeng, P.L.-G. Chong, Effect of ethanol-induced lipid interdigitation on the membrane solubility of Prodan, Acдан, and Laurdan, *Biophys. J.* 68 (1995) 567–573.
- [15] P. Nambi, E.S. Rowe, T.J. McIntosh, Studies of the ethanol-induced interdigitated gel phase in phosphatidylcholines using the fluorophore 1,6-diphenyl-1,3,5-hexatriene, *Biochemistry* 27 (1988) 9175–9182.
- [16] Z.V. Leonenko, D.T. Cramb, Revisiting lipid – general anesthetic interactions (I): thinned domain formation in supported planar bilayers induced by halothane and ethanol, *Can. J. Chem.* 82 (2004) 1128–1138.
- [17] F.W.S. Stetter, T. Hugel, The nanomechanical properties of lipid membranes are significantly influenced by the presence of ethanol, *Biophys. J.* 104 (2013) 1049–1055.
- [18] J.M. Vanegas, M.F. Contreras, R. Faller, M.J. Longo, Role of unsaturated lipid and ergosterol in ethanol tolerance of model yeast biomembranes, *Biophys. J.* 102 (2012) 507–516.
- [19] J.M. Vanegas, R. Faller, M.L. Longo, Influence of ethanol on lipid/sterol membranes: phase diagram construction from AFM imaging, *Langmuir* 26 (2010) 10415–10418.
- [20] J.T. Marquês, A.S. Viana, R.F.M. De Almeida, Ethanol effects on binary and ternary supported lipid bilayers with gel/fluid domains and lipid rafts, *Biochim. Biophys. Acta* 1808 (2011) 405–414.
- [21] E. London, How principles of domain formation in model membranes may explain ambiguities concerning lipid raft formation in cells, *Biochim. Biophys. Acta* 1746 (2005) 203–220.
- [22] S.L. Veatch, S.L. Keller, Seeing spots: complex phase behavior in simple membranes, *Biochim. Biophys. Acta* 1746 (2005) 172–185.
- [23] R.M. Pines, H.F. Costa, A.G.M. Ferreira, I.M.A. Fonseca, Viscosity and density of water + ethyl acetate + ethanol mixtures at 298.15 and 318.15 K and atmospheric pressure, *J. Chem. Eng. Data* 52 (2007) 1240–1245.
- [24] N.L. Thompson, H.M. McConnell, T.P. Burghardt, Order in supported phospholipid monolayers detected by the dichroism of fluorescence excited with polarized evanescent illumination, *Biophys. J.* 46 (1984) 739–747.
- [25] A. Anantharam, B. Onoa, R.H. Edwards, R.W. Holz, D. Axelrod, Localized topological changes of the plasma membrane upon exocytosis visualized by polarized TIRFM, *J. Cell Biol.* 188 (2010) 415–428.
- [26] V. Kiessling, M.K. Domanska, L.K. Tamm, Single SNARE-mediated vesicle fusion observed in vitro by polarized TIRFM, *Biophys. J.* 99 (2010) 4047–4055.
- [27] J. Oreopoulos, C.M. Yip, Probing membrane order and topography in supported lipid bilayers by combined polarized total internal reflection fluorescence–atomic force microscopy, *Biophys. J.* 96 (2009) 1970–1984.
- [28] J. Oreopoulos, R.F. Epanand, R.M. Epanand, C.M. Yip, Peptide-induced domain formation in supported lipid bilayers: direct evidence by combined atomic force and polarized total internal reflection fluorescence microscopy, *Biophys. J.* 98 (2010) 815–823.
- [29] D.M. Carter Ramirez, Z.J. Jakubek, Z. Lu, W.W. Ogilvie, L.J. Johnston, Changes in order parameters associated with ceramide-mediated membrane reorganization measured using pTIRFM, *Langmuir* 29 (2013) 15907–15918.
- [30] J.H. Davis, J.J. Clair, J. Juhasz, Phase equilibria in DOPC/DPPC-d62/cholesterol mixtures, *Biophys. J.* 96 (2009) 521–539.
- [31] S.C.D.N. Lopes, M.A.R.B. Castanho, Overview of common spectroscopic methods to determine the orientation/alignment of membrane probes and drugs in lipidic bilayers *Curr. Org. Chem.* 9 (2005) 889–898.
- [32] T.T. Mills, S. Tristram-Nagle, F.A. Heberle, N.F. Morales, J. Zhao, J. Wu, G.E.S. Toombes, J.F. Nagle, G.W. Feigenson, Liquid–liquid domains in bilayers detected by wide angle X-ray scattering, *Biophys. J.* 95 (2008) 682–690.
- [33] S.L. Veatch, O. Soubias, S.L. Keller, K. Gawrisch, Critical fluctuations in domain-forming lipid mixtures, *Proc. Natl. Acad. Sci.* 104 (2007) 17650–17655.
- [34] F.S. Ariola, D.J. Mudaliar, R.P. Walvick, A.A. Heikal, Dynamics imaging of lipid phases and lipid-marker interactions in model biomembranes, *Phys. Chem. Chem. Phys.* 8 (2006) 4517–4529.
- [35] P.W. Livanec, H.A. Huckabay, R.C. Dunn, Exploring the effects of sterols in model lipid membranes using single molecule orientations, *J. Phys. Chem. B* 113 (2009) 10240–10248.
- [36] K.C. Song, P.W. Livanec, J.B. Klauda, K. Kuczera, R.C. Dunn, W. Im, Orientation of fluorescent lipid analogue BODIPY-PC to probe lipid membrane properties: insights from molecular dynamics simulations, *J. Phys. Chem. B* 115 (2011) 6157–6165.
- [37] C.D. Blanchette, W.-C. Lin, C.A. Orme, T.V. Ratto, M.L. Longo, Domain nucleation rates and interfacial line tensions in supported bilayers of ternary mixtures containing galactosylceramide, *Biophys. J.* 94 (2008) 2691–2697.
- [38] L.J. Johnston, Nanoscale imaging of domains in supported lipid membranes, *Langmuir* 23 (2007) 5886–5895.
- [39] M.A. Bos, J.M. Klein, Determination of the orientation distribution of adsorbed fluorophores using TIRF. II. Measurements on porphyrin and cytochrome c, *Biophys. J.* 68 (1995) 2566–2572.
- [40] F.S. Ariola, Z. Li, C. Cornejo, R. Bittman, A.A. Heikal, Membrane fluidity and lipid order in ternary giant unilamellar vesicles using a new Bodipy-cholesterol derivative, *Biophys. J.* 96 (2009) 2696–2708.
- [41] T. Baumgart, G. Hunt, E.R. Farkas, W.W. Webb, G.W. Feigenson, Fluorescence probe partitioning between L_0/L_d phases in lipid membranes, *Biochim. Biophys. Acta* 1768 (2007) 2182–2194.
- [42] Y. Kurniawan, K.P. Venkataraman, C. Scholz, G.D. Bothun, n-Butanol partitioning and phase behavior in DPPC/DOPC membranes, *J. Phys. Chem. B* 116 (2012) 5919–5924.
- [43] R.C. Lyon, J.A. McComb, J. Schreurs, D.B. Goldstein, A relationship between alcohol intoxication and the disordering of brain membranes by a series of short-chain alcohols, *J. Pharmacol. Exp. Ther.* 218 (1981) 669–675.
- [44] M.J. Pringle, K.B. Brown, K.W. Miller, Can the lipid theories of anesthesia account for the cutoff in anesthetic potency in homologous series of alcohols? *Mol. Pharmacol.* 19 (1981) 49–55.
- [45] P.W. Westerman, J.M. Pope, N. Phonphok, J.W. Doane, D.W. Dubro, The interaction of n-alkanols with lipid bilayer membranes: a 2H NMR study, *Biochim. Biophys. Acta* 939 (1988) 64–67.
- [46] S. Kwak, E. Brief, D. Langlais, N. Kitson, M. Lafleur, J. Thewalt, Ethanol perturbs lipid organization in models of stratum corneum membranes: an investigation combining differential scanning calorimetry, infrared and 2H NMR spectroscopy, *Biochim. Biophys. Acta* 1818 (2012) 1410–1419.
- [47] K.P. Armendariz, H.A. Huckabay, P.W. Livanec, R.C. Dunn, Single molecule probes of membrane structure: orientation of BODIPY probes in DPPC as a function of probe structure, *Analyst* 137 (2012) 1402–1408.